



**HAL**  
open science

## Complexity in earthquake sequences controlled by multi-scale heterogeneity in fault fracture energy

Hideo Aochi, Satoshi Ide

► **To cite this version:**

Hideo Aochi, Satoshi Ide. Complexity in earthquake sequences controlled by multi-scale heterogeneity in fault fracture energy. *Journal of Geophysical Research: Solid Earth*, 2009, 114 (B03305), 13 p. 10.1029/2008JB006034 . hal-00502710

**HAL Id: hal-00502710**

**<https://brgm.hal.science/hal-00502710>**

Submitted on 15 Jul 2010

**HAL** is a multi-disciplinary open access archive for the deposit and dissemination of scientific research documents, whether they are published or not. The documents may come from teaching and research institutions in France or abroad, or from public or private research centers.

L'archive ouverte pluridisciplinaire **HAL**, est destinée au dépôt et à la diffusion de documents scientifiques de niveau recherche, publiés ou non, émanant des établissements d'enseignement et de recherche français ou étrangers, des laboratoires publics ou privés.

1 **Complexity in earthquake sequences controlled by**  
2 **multi-scale heterogeneity in fault fracture energy**

3  
4 Hideo Aochi

5 Land Planning and Natural Risks Division, BRGM, 3 avenue Claude Guillemin,  
6 Orléans 45060 Cedex, France. ([h.aochi@brgm.fr](mailto:h.aochi@brgm.fr))

7  
8 Satoshi Ide

9 Earth and Planetary Science, The University of Tokyo, 7-3-1 Hongo, Bunkyo-ku,  
10 Tokyo 113-0033, Japan. ([ide@eps.s.u-tokyo.ac.jp](mailto:ide@eps.s.u-tokyo.ac.jp))

11  
12 **Abstract**

13 A series of dynamic rupture events under constant tectonic loading is simulated on a  
14 fault with multi-scale heterogeneity and a stochastic rupture initiation process. The  
15 fracture energy of the fault plane is assumed to have multi-scale heterogeneous  
16 distribution using fractal circular patches. The stochastic rupture initiation process as a  
17 function of the accumulated stress is introduced in order to take account of unknown  
18 smaller-scale heterogeneity and variability. Five realizations of a statistical spatial  
19 distribution of fracture energy (fault heterogeneity maps) are tested for the simulations  
20 of earthquake sequences during a few seismic cycles. The diversity of earthquake  
21 sequences is principally controlled by the spatial distribution of the patches. The effect

1 of dynamic rupture appears in the residual stress after the characteristic events due to  
2 their directivity and this localizes the subsequent sequences. Although the characteristic  
3 earthquakes occur rather regularly in time and similarly in different seismic cycles,  
4 some irregular behavior is found, based on the heterogeneity maps and the randomness  
5 of the preceding earthquake sequence, leading to a visible anomaly in the seismicity.  
6 Such anomalies are not predicable, but understandable through the analysis of the  
7 considered earthquakes during the cycle. The similarity and the diversity simulated in  
8 this study, governed by the structure of an inherent distribution of multi-scale  
9 heterogeneity, suggests the importance of the pre-existing heterogeneity field along the  
10 fault for the appearance of earthquake sequences, including those that are characteristic.

## 11 **1. Introduction**

12  
13 Most numerical studies of earthquake source dynamics have been based on a fixed  
14 observation scale, namely the assumption of characteristic, or fixed-scale, fault  
15 parameters for a target event; while there are few examples considering multi-scalability  
16 of fault parameters (e.g. Andrews, 1976; Aochi and Ide, 2004; Ide and Aochi, 2005;  
17 Andrews, 2005). Some spatial heterogeneity on a fault plane is often given in terms of  
18 stress and/or fault strength to explain the complexity of event (e.g. Mikumo and  
19 Miyatake, 1979; Olsen et al., 1997; Fukuyama and Madariaga, 1998; Guatteri et al.,  
20 2003; Oglesby and Day, 2005; Ripperger et al., 2007; and many others). The  
21 heterogeneous stress field has recently been also attributed to the complex fault  
22 geometry due to the irregular topography with respect to a tectonic force (e.g. Aochi  
23 and Fukuyama, 2002) and/or the history of past events (e.g. Duan and Oglesby, 2005;  
24 Shaw and Dieterich, 2007). As is natural, no detail smaller than an assumed model grid

1 size can be taken into account.

2 Recently, Ide and Aochi (2005) pointed out that multi-scale heterogeneity is essential in  
3 modeling wide-scale self-similarity of the earthquake source process (e.g., Ide and  
4 Beroza, 2001; Uchide and Ide, 2007), which cannot be modeled by a viewpoint at a  
5 single scale. Such multi-scale heterogeneity should be able to be introduced in the  
6 fracture energy of the fault surface, or simply in the critical slip distance  $D_c$  of a  
7 slip-weakening law considering that fault strength is approximately constant and  
8 independent of the scales. The fracture energy is estimated as from  $1 \text{ J/m}^2$  in laboratory  
9 experiments (Atkinson, 1984; Ohnaka, 2003) to  $1 \text{ MJ/m}^2$  for large earthquakes (Beroza  
10 and Spudich, 1988; Ide 2002). Linearly increasing  $G_c$  in a uniformly strained medium  
11 produces a self-similar rupture propagation and thus explains the scale-independency of  
12 rupture propagation velocity and slip velocity within the ruptured area (e.g. Andrews,  
13 1976; Aochi and Ide, 2004). Such scaling in fracture energy can be explained by the  
14 fractal nature of fault surface roughness (Matsu'ura et al., 1992; Ohnaka, 2003; Ide and  
15 Aochi, 2005), while there are other possible interpretations such as purely mechanical  
16 effects between cracks (Yamashita and Fukuyama, 1996) or anelastic effects off the  
17 rupture plane (Andrews, 2005). Our model in this study is based on the former, namely  
18 that fracture energy is regarded as an intrinsic parameter given in advance. On a fault  
19 with a hierarchical  $G_c$  distribution, a rupture propagates self-similarly and stops without  
20 special mechanisms because the rupturing area is always covered by an area of larger  $D_c$   
21 except for the largest characteristic earthquake of the system (Ide and Aochi, 2005).  
22 This does not mean that other heterogeneity in stress or other parameters in the friction  
23 law are not important; however, there are few studies focusing on the fracture energy  
24 and, therefore, it should be worth studying. The importance of this scaling problem is

1 shown by its influence on the radiated seismic waves from a fault (e.g. Mai et al., 2006).  
2 This paper considers how this multi-scale heterogeneity can be taken into account when  
3 discussing, not only single events of different magnitudes, but also a sequence of such  
4 events. The conclusion inferred from the study of Ide and Aochi (2005) on single events  
5 is that a perturbation (rupture initiation) on any small heterogeneity remains as a local  
6 event of small magnitude with a few exceptions that lead to the rupture of the entire  
7 system (a so-called characteristic event) showing a cascade-like rupture growth  
8 (Ellsworth and Beroza, 1995). Although each event is perfectly governed by the  
9 physical law, the system behavior appears stochastic because of the uncertainty of the  
10 initiation process. As emphasized in Ide and Aochi (2005), a rupture can initiate from a  
11 part much smaller than its final size and such an initiation often becomes unstable due  
12 to local fluctuations in stress or strength, which are not described in the deterministic  
13 simulation of the rupture propagation. Thus the initiation process requires a stochastic  
14 process representing unknown microscopic heterogeneities. This process is controlled  
15 by deterministically calculated macroscopic parameters, such as the average stress level.  
16 Besides the studies of earthquake dynamic rupture, there are many previous works on  
17 simulating seismicity. One end member, as represented by Otsuka (1971) and Bak and  
18 Tang (1989), for instance, is based on a simple mechanical model of stress release on a  
19 concerned grid and stress redistribution on the surrounding grid. Although these models  
20 show the characteristics of self-organized criticality, such as a wide range of events  
21 under no explicit spatial inhomogeneity, the governing system has only the  
22 nearest-neighbor interaction of a spring between two discretized blocks and may not be  
23 a proper approximation of a continuum medium where earthquakes occur. Thus another  
24 kind of mechanical model based on fracture mechanics in an elastic medium has been

1 developed (Mikumo and Miyatake, 1979; Yamashita, 1993; Rice, 1993; Ben-Zion and  
2 Rice, 1993; Lapusta et al., 2000; Zöller et al., 2005b; Hillers et al., 2006). As a crack  
3 evolves deterministically according to the elastic response and stress-displacement  
4 constitutive relation on the crack, the system approaches a limit cycle unless the grid  
5 resolution is insufficient with respect to a characteristic scale determined by the fault  
6 constitutive relation (Rice, 1993). In this case, some other heterogeneity in the  
7 parameters is required to generate the complexity of the seismicity in the continuum  
8 medium as in the dynamic rupture process of single events. Numerical efforts have been  
9 made to treat more complex heterogeneity and a large number of degrees of freedoms  
10 have been added to simulate a wide range of earthquakes. As we focus on the effect of  
11 dynamic earthquake events and so-called “asperities”, we will adopt a friction law that  
12 does not allow any aseismic slip during the simulation. There exist some studies, e.g.  
13 Lapusta et al. (2000) and Lapusta and Liu (2008), which simulate sequences of dynamic  
14 events and interseismic creeping within a single computational procedure and suggest  
15 that the interseismic processes may significantly change fault stress/strength conditions  
16 before earthquakes and, therefore, that it influences dynamic rupture processes.  
17 However, in most studies, smaller scales, which cannot be deterministically described  
18 on a model element, are not considered. In this case, these simulations are always  
19 deterministic regardless of the variety of event sequences. The aim of this paper is to  
20 take into account such small-scale instabilities and their consequences on macroscopic  
21 earthquake sequences.

22 In this paper, we first explain the concept of a multi-scale heterogeneous fault according  
23 to Ide and Aochi (2005) and propose a process of stochastic rupture initiation controlled  
24 by a temporal evolution of stress. Then we examine five different distributions of

1 fracture energy (fault heterogeneity maps) randomly generated according to our rules  
2 and then carry out the numerical simulation of earthquake sequences during a hundred  
3 years. Each of these sequences is physically simulated using elasto-dynamics for a  
4 rupture event. Finally we analyze the simulation results in terms of their spatio-temporal  
5 characteristics. We are interested especially in how characteristic events occur in the  
6 sequence.

## 7 **2. Model**

### 8 ***2.1 Multi-scale heterogeneous fault description***

9  
10 Let us consider a single isolated square fault segment under a far-field tectonic loading.  
11 Our fault model is principally based on the previous one of Ide and Aochi (2005), in  
12 which circular patches of different sizes are distributed randomly on a fault plane as  
13 illustrated in Figure 1. The number of patches follows a fractal distribution of the  
14 size-number relation. Letting  $N_n$  be the number of the patches of the  $n$ -th order with a  
15 radius  $r_n$ :

$$16 \quad r_n = 2^n r_0 \quad (1)$$

17 then we set:

$$18 \quad N_n = 2^{-Dn} N_0 \quad (2)$$

19 where the fractal dimension is chosen as  $D = 2$ . There are 16384 ( $= N_0$ ) 0-th order  
20 patches of the smallest size, while one for the 7th order patch whose radius is  $2^7 = 128$   
21 times larger than the smallest ones. Additionally we introduce an 8<sup>th</sup>-order patch with an  
22 appearance probability of 0.25. In this paper, we call these patches and patch  
23 distribution simply as the heterogeneity and fault heterogeneity map, respectively. It

1 should be noted that, as explained in the later sections, no other intrinsic heterogeneity  
 2 is assumed in our model, namely heterogeneity in the stress field is generated naturally  
 3 according to the earthquake history and stress loading is uniform over the fault. .

4 Next it is assumed that each patch has fracture energy  $G_c$  proportional to its radius:

$$5 \quad G_c \propto r_n^2, \quad (3)$$

6 so that the smallest patches represent the weakest points. A simple slip-weakening  
 7 friction law between shear stress  $\tau$  and fault slip  $\Delta u$  is introduced to govern the  
 8 rupture process on the fault during slipping:

$$9 \quad \tau(\Delta u) = \Delta\tau_b(1 - \Delta u / D_c)H(1 - \Delta u / D_c) + \tau_r, \quad (4)$$

10 where the parameters  $\Delta\tau_b$  and  $D_c$  are called breakdown strength drop and critical  
 11 slip distance and  $H(\cdot)$  is the Heaviside function.  $\tau_r$  represents a level of so-called  
 12 dynamic friction (residual stress), but hereafter  $\tau_r = 0$  is assumed without loss of  
 13 generality for a planar fault problem because we discuss the deviate stress. The fault  
 14 strength (static friction) is thus written as  $\Delta\tau_b + \tau_r$  when the fault is not sliding. As is  
 15 mentioned later, an immediate healing process is assumed. In this formulation, fracture  
 16 energy is simply written by  $G_c = \Delta\tau_b \cdot D_c / 2$ . We assume  $\Delta\tau_b$  uniform everywhere at  
 17 every scale (= 5 MPa) to simplify the problem so that the scale-dependent parameter of  
 18 interest is  $D_c$ . Hereafter we will discuss this parameter  $D_c$  instead of the fracture  
 19 energy  $G_c$ . The importance of the linear scale dependence of  $D_c$  has been pointed out  
 20 by different researchers (e.g. Andrews, 1976; Matsu'ura et al., 1992; Ohnaka, 2003).  
 21 This scale dependence is a necessary condition for the self-similarity of the dynamic  
 22 earthquake rupture between small and large earthquakes, which is strongly implied by

1 laboratory experiments and seismological analyses. The problem had been the degree of  
2 variation in  $D_c$  for a single system. Integrating the concept of Matsu'ura et al. (1992)  
3 and Ohnaka (2003) that  $D_c$  originates from the topology of fault surface, our previous  
4 work (Ide and Aochi, 2005), consisting of Equations (1) to (4), has successfully shown  
5 that various sizes of earthquakes occur on a single fault system having a  $D_c$   
6 distribution.

7 In this study, the dimension of the fault area is  $16.4 \times 16.4 \text{ km}^2$  surrounded by an  
8 unbreakable barrier, which implies that this fault is isolated from the outside. This fault  
9 is subdivided into  $4096 \times 4096$  elements which cannot currently be treated directly by  
10 our numerical scheme. Thus, as explained in the next section, we dynamically adjust the  
11 grid size of the calculation to the scale where the rupture is progressing during each  
12 earthquake. We generate five different distributions of circular patches as shown in  
13 Figure 2. The location of each patch is randomly determined within the whole fault  
14 plane. The minimum  $D_c$  is 0.25 mm. It is noted that the largest patch does not always  
15 appear as its appearance probability equals 0.25. This fault is also charged by a constant  
16 far-field tectonic loading, which controls stochastic initiation process as explained in a  
17 later section. Thus the complexity arises both from the stochastic growth of earthquake  
18 rupture and from the stochastic rupture initiation process.

## 19 ***2.2 Simulation of the dynamic rupture stage***

20  
21 In this section, we explain the part of the deterministic calculation of this simulation  
22 based on the dynamic and static response in a homogeneous, infinite elastic medium.  
23 Once rupture is initiated somewhere on the fault, we calculate the spontaneous dynamic  
24 process using a boundary integral equation method (BIEM: Fukuyama and Madariaga,

1 1995, 1998) and a renormalization technique (Aochi and Ide, 2004), which allows us to  
2 follow the growth process of the rupture by changing the grid size until the arrest of  
3 rupture by conserving the released seismic moment and the fracture energy on the  
4 concerned area. The rupture initiation at the initial step is given by a finite circular  
5 crack; this effect disappears rapidly after the renormalization process [See Figures 2 and  
6 4 in Aochi and Ide (2004)]. From the viewpoint of larger scales, the dynamic rupture  
7 process appears to begin as a point in our configuration. The BIEM calculation is  
8 always carried out on the unit grid with  $64 \times 64$  boundary elements by using a  
9 technique of two-dimensional fast Fourier transforms. According to the definition of the  
10 BIEM, nothing happens outside the physical model region, i.e. we do not need to  
11 consider it. An unbreakable barrier theoretically represents the condition that fault slip  
12 always equals zero.

13 Once a dynamic rupture begins (see the next section on how it is triggered), the stress  
14 drops in the ruptured area with fault slip according to Equation (4) while stress  
15 accumulates in the surrounding area according to elasto-dynamics, calculated by the  
16 BIEM. During this process, the fault slip is triggered at each grid point once the applied  
17 shear stress exceeds the fault strength ( $\Delta\tau_b + \tau_r$ ). This means that there remains in  
18 principle a possibility that dynamic stress perturbation may cause a rupture at distance  
19 away from the rupture front, as our model is intrinsically heterogeneous at all scales.  
20 However, a triggered event of significant size is rarely observed in the following  
21 simulation. This is because, as we will see later, the probability for a rupture to grow  
22 logarithmically decreases with size and also because such instabilities may soon  
23 coalesce with the dominant rupture area even if it exists. Thus, although this mechanism  
24 could be important when discussing high-frequency seismic wave radiation and

1 dynamic triggering in a more complex fault system, its influence is limited for the  
2 macroscopic view of rupture growth on a single plane, which we aim to discuss in this  
3 paper. Once all the grids are complete at a scale where the simulation is progressing, the  
4 dynamic rupture simulation of one event finishes. At the end of each dynamic rupture  
5 simulation, we calculate the static stress change due to the event. To simplify the  
6 numerical procedure, the near-field stress change is calculated based on the scale where  
7 the rupture has terminated, while the far-field stress is rapidly calculated on the  
8 large-scale grids by using a renormalization technique. This is a good enough  
9 approximation since the detail of the slip distribution mostly perturbs the region close to  
10 the ruptured area and the change in the stress field is gradual at distance. This  
11 significantly speeds up the process.

12 The slip-weakening law in (4) has no healing mechanism, but it is unlikely that the  
13 ruptured area remains weak a long time after the event. For simplicity, we, therefore,  
14 assume that the fault is healed immediately after arrest, to its original strength value and  
15 that it keeps the same value of fracture energy, or  $D_c$ , resetting  $\Delta u$  to be zero in  
16 Equation (4). The first event occurs under a uniform stress field, but the stress field  
17 evolves to be heterogeneous through the ongoing seismicity. During the sequences, the  
18 stress values may even become negative in our numerical system due to the  
19 overshooting effect of the dynamic rupture process. However, “back slip” is prohibited,  
20 as  $\tau_r$  in Equation (4) is not really zero but high enough to suppress backward motion  
21 in nature.

### 22 ***2.3 Stochastic initiation process and system evolution***

23  
24 The initiation criterion for each event is a fundamental assumption in this study. We

1 introduce a stochastic description reflecting unknown heterogeneity and a macroscopic  
2 stress field, which is the available information in the above framework. Laboratory  
3 experiments suggest a Weibull-type distribution for the strength distribution of rock  
4 material (e.g. Yamaguchi and Nishimatsu, 1967) and previous numerical studies  
5 adopted such a strength distribution (e.g. Mikumo and Miyatake, 1978, 1979). However,  
6 this study assumes uniform fault strength and introduces prescribed fracture energy at  
7 each point on the fault as the rupture process is deterministically described by a fault  
8 constitutive relation and elasto-dynamics. Thus, we need another way to model the  
9 fragility of each point with respect to the given fracture criterion and stress condition.

10 As shown in numerous deterministic simulations, giving a small instability to a  
11 nucleation area with some finite size allows spontaneous dynamic rupture propagation  
12 even if the stress is moderately loaded on the fault system. This is often discussed by  
13 some normalized parameter between stress, strength or fracture energy (e.g. Das and  
14 Aki, 1977; Shibazaki and Matsu'ura, 1998; Madariaga and Olsen, 2000). These all  
15 imply that there remains an arbitrary selection of the nucleation points with respect to  
16 the stress field and it is well known that this significantly affects the rupture history and  
17 the wave radiation (e.g. Guatteri et al., 2003; Aochi et al., 2006). No quantitative  
18 description of the selection of such an initiation process has been established, as this  
19 may be physically related to the microscopic heterogeneity that we cannot describe  
20 deterministically. In this paper, we thus assume that this selection is stochastic with a  
21 function of accumulated stress and propose to approximate it by a Weibull distribution  
22 function. The selection, i.e. the probability of rupture  $P$  of any patch of the minimum  
23 size under the applied stress  $\tau$  within a fixed duration, is written using a Weibull  
24 distribution:

$$P(\tau; k, \lambda) \propto (k/\lambda)(\tau/\lambda)^{k-1} \exp(-(\tau/\lambda)^k), \quad (5)$$

1 where  $k$  (shape parameter) and  $\lambda$  (scale parameter) determine the shape of the  
 2 distribution and the characteristic stress level related to the maximum probability,  
 3 respectively. This probability  $P$  is defined to be zero when  $\tau \leq 0$  and a condition of  
 4  $\tau > 5$  does not exist in our context. Equation (5) might be replaced by another  
 5 functional form, but the merit of using this function is that it is sufficient to study  $k$   
 6 since  $\lambda$  is taken equal to the assumed peak strength ( $\lambda = 5$  MPa). Figure 3 shows this  
 7 function for different values of  $k$ . This qualitatively matches our hypothesis, where the  
 8 probability is effectively zero at very low stresses and increases with the external stress  
 9 until the supposed strength. A large value of  $k$  produces a narrow peak around  $\lambda$ ,  
 10 which makes rupture initiation sensitive to the macroscopic stress concentration. In  
 11 contrast, with a small  $k$ , rupture initiation under low stress is more likely, which means  
 12 that the microscopic stress perturbation on any patch is relatively independent of the  
 13 initiation probability that is controlled mainly by surrounding macroscopic stress field.  
 14 In the presence of tectonic loading, stress state and the probability of event occurrence  
 15 depends on time. Adjusting the far field stress loading rate, we may control the  
 16 recurrence time of seismic cycles. Event frequency is related to Equation (5). To  
 17 normalize this equation in a seismic cycle, we suppose a roughly characteristic event of  
 18 this fault (Mw about 6) every  $T$  year. The standard Gutenberg-Richter law then  
 19 predicts  $10^{(6-M)}$  events of magnitudes greater than  $M$  during the period  $T$ .  
 20 Remembering that the minimum simulated event appears around magnitude  $M = 1$   
 21 corresponding the smallest patches on the fault system, we assume that all the initiation  
 22 points are triggered at least once during these  $T$  years. The average event interval is  
 23

1 then  $t_{int} = T$  (years)/16384 (events), and the mean probability of events is  $P_{event} =$   
 2  $t_{int}^{-1}$  per unit time. Namely we normalize Equation (5) so as to satisfy the following  
 3 relation taking a stress value of 3MPa as reference:

$$4 \quad N_{min} \times P(\tau = 3 \text{ MPa}; k, \lambda) = P_{event}. \quad (6)$$

5 However, this normalization is based on the assumption of a uniform stress field of 3  
 6 MPa. As we will see in the following sections, stress field evolves with tectonic loading  
 7 and event sequences and hence the stress applied on the system is not stationary. More  
 8 precisely, it is lower during most of the period because the characteristic events release  
 9 the entire accumulated stress at once. As a consequence, we will see that the simulated  
 10 seismicity is much lower than expected. We finally assume that the tectonic stress  
 11 loading for each time step,  $\Delta\tau_{tectonic}$ , is constant, namely stress builds up to 3 MPa,  
 12 taken as the reference above, during  $T$ . The parameters are summarized in Table 1.

13 We note that the above procedure selects either no hypocenter or one hypocenter at each  
 14 time step. If no hypocenter is selected, we advance in time. If one hypocenter is selected,  
 15 this defines the initial model space at the finest scale where we begin a dynamic  
 16 simulation. In the dynamic rupture simulations, an instantaneous strength drop is given  
 17 at the beginning on a small area within a selected smallest patch. Namely the strength is  
 18 forced to be zero in Equation (4). Once selected, this initial process has a positive stress  
 19 drop so that the rupture progresses more or less spontaneously according to the current  
 20 boundary conditions.

21

22

### 3. Simulation results

We execute the simulations for five different fault heterogeneity maps (Figure 2) based on the above procedure. The parameters are given in Table 1, considering a tectonically active zone (on average a M6.5 event every 20 years). The parameters of the Weibull's function are chosen after studying the results of our preliminary run. We discuss the sensitivity to the parameters in a later section. We begin the simulation with a uniform stress of 3.5 MPa expecting the first characteristic earthquake to occur early in all the simulation; this warming-up period (cycle 0) is not taken into account in subsequent discussions. Here the characteristic earthquake is defined as the rupture process propagating on the whole fault area and being stopped by the barriers outside of the modeled region. Such an event completely releases the accumulated stress on the fault. We run each simulation for a hundred years, by running the stochastic initiation process every hour and by simulating the dynamic rupture process for a time step for a minimum 0.33 ms. This takes more than a week on a quad-core machine, although one earthquake is usually simulated within a few minutes. In the following section, we first discuss the statistical aspects of the earthquake sequences and then watch the details of the rupture process occurring in the simulation, from deterministic point of view.

#### 3.1 Earthquake sequences with time

Figures 4 and 5 show the earthquake sequences with time for a hundred years for five fault heterogeneity maps. Characteristic events (Mw 6.4-6.5) repeat constantly in all cases with an average recurrence interval of about 20 years after a certain number of earthquakes have occurred. As reported in Table 2, the variation in the recurrence

1 interval of characteristic earthquakes is relatively small. The difference between  
2 maximum and minimum recurrence times within each simulation is less than 5 % of the  
3 average recurrence time for maps (1) to (3), and 7 % and 13 % for (4) and (5),  
4 respectively. This originates from the internal effect of the stochastic rupture initiation,  
5 including the choice of random numbers and the subsequent earthquake histories along  
6 the fault. More interestingly, the maximum difference in the average recurrence time  
7 according to the fault heterogeneity maps is rather large, 1.89 years, namely the  
8 diversity due to the maps is larger than the fluctuation (randomness) within each  
9 simulation except for (5). This indicates the importance of the geometrical distribution  
10 of the patches (fault heterogeneity), although all the maps are realizations of the same  
11 statistical model. The uniqueness of (5) is clear in the fault heterogeneity map where the  
12 maximum patch is accidentally missed.

13 It is found that the number of earthquakes accelerates with time and the maximum  
14 magnitude also increases. This is controlled by the external stress level. First, the  
15 increase of stress level raises the probability of the rupture initiation following Equation  
16 (5) so that it eases the appearance of earthquakes with time. On the other hand, the  
17 dominance of large events indicates that larger earthquakes require higher stress loading  
18 over a large area, while small earthquakes can occur within a localized stress  
19 accumulation. Higher background stress enhances patch interaction and growth to  
20 become a large event.

21 It is not surprising that no earthquake appears just after a characteristic event. This is  
22 because the stress is completely released across the entire fault and it takes time to  
23 recover enough stress to lead to a new earthquake. This is a common feature in previous  
24 studies, which do not introduce any specific mechanisms for delayed rupture, relaxation

1 of the medium, pore fluid flow and so on (e.g. Zöller et al., 2005a).

2

### 3 **3.2 Earthquake size distribution**

4 In this section, we report the size distribution of the earthquakes. As already clearly  
5 shown in Figure 4, the greater tectonic stress accumulated with time, the larger the  
6 earthquake that appears. This indicates that the larger earthquakes require widely  
7 accumulated stress. On other hand, small earthquakes easily occur at any time without  
8 growing to large events, mainly because they are controlled by small-scale  
9 heterogeneities that are recovered relatively quickly. Figure 6 shows the size-frequency  
10 relation for the cumulative number of earthquakes within each simulation. The  
11 characteristic events of around M6.5 are shifted from the scaling relation of smaller  
12 earthquakes. We then find that most of the seismic cycles in all the simulations briefly  
13 show a linear Gutenberg-Richter relation, while the ones of simulation (4) and (5) show  
14 significantly curved relations with dominant magnitudes around 3 [there is also a small  
15 curvature in the relation for simulation (3)]. In the latter case, it should be noted that the  
16 number of earthquakes also increases. This means that there should be something  
17 characteristic at this scale to break the scaling relation. Many earthquakes cannot grow  
18 larger than this size. This feature can be understood deterministically by detailed  
19 analysis of the earthquake sequences (See section 3.4)

20 The absence of aftershocks has already been reported in Figures 4 and 5. In nature, the  
21 characteristic event accompanies many aftershocks, which often show a  
22 Gutenberg-Richter size-frequency relation. On the other hand, it is also known that such  
23 relations are visible in any time period during a seismic cycle, even for background

1 seismicity. Therefore it is not surprising that a Gutenberg-Richter behavior appears  
2 without aftershocks.

### 3 4 **3.3 Spatial pattern of sequences**

5 The spatial patterns of seismicity in Figure 7 have some interesting features. First,  
6 although the seismicity is greatly distributed, some concentrations and/or gaps are found.  
7 From the macroscopic view of the whole fault area, the seismicity is located more on  
8 the upper section of the fault in (1) and (2) and located on the lower section in (3), for  
9 example. On the other hand, in some cycles such as indicated in green for (4) and purple  
10 for (5), the sequences sometimes leave a gap in certain areas and in the surrounding  
11 regions many more earthquakes are found. In this case, the number of earthquakes also  
12 increases (Figure 5) and some dominant earthquake size appears (Figure 6). Both  
13 phenomena should be the result of some physical process of earthquake ruptures  
14 regardless of the randomness of the rupture initiation. On the other hand, we find that  
15 the hypocenters of the characteristic earthquakes are sometimes close to one other, as  
16 four events in (1) and all events in (2), for example. In (3), the hypocenters are divided  
17 into two different areas. We will next discuss these similarities and the complexity by  
18 considering in detail the process of earthquake ruptures.

### 19 20 **3.4 Stress field evolution**

21 The upper and lower rows of Figure 8 respectively show the stress field before and after  
22 every characteristic earthquake in the simulations. More exactly, the upper row

1 represents the final stress of the precedent earthquake and the lower row is the final  
2 stress when the characteristic earthquakes have finished. The evolution of the stress  
3 field pattern can be classified into two groups: rather homogeneous evolution  
4 represented by (1) and (2) of Figure 8, and inhomogeneous evolution due to some  
5 visible ruptured area of intermediate magnitude earthquakes, especially observed in the  
6 third cycle of (4), for example. Comparing Figure 8 with the fault heterogeneity and  
7 seismicity (Figures 2 and 7), we can find how each system becomes ready to rupture the  
8 whole area, or the largest patch. Such instability requires some large areas with almost  
9 complete stress drop. These areas may be formed dynamically within a single event as a  
10 cascade, which we may call dynamic nucleation, or it may happen during many  
11 precedent earthquakes as in a quasi-static nucleation.

12 The fault heterogeneity maps (1) and (2) (Figure 2) are typical examples of the former  
13 case. Namely the patch distribution allows a cascade-like rupture growth from the  
14 smallest patch to the largest one (Ide and Aochi, 2005). A small perturbation can easily  
15 grow to a characteristic event without a large quasi-static nucleation area. Only a small  
16 number of earthquakes occur leaving a clear gap between magnitude 4 and 6.5 in the  
17 magnitude-frequency relation. This also explains the closeness of the hypocenters of the  
18 characteristic events. In map (1), a cascade-like growth must propagate into the largest  
19 patch located in the right upper corner. The only exception is a rupture that begins far  
20 from this patch at the end of the first cycle (star in purple in Figure 7), the rupture  
21 process takes longer, by about 40 %, to propagate along the whole fault area, than in the  
22 other simulations. Despite the similarity of the initial scenario, slightly different  
23 behavior can be observed for the characteristic event. The rupture may initiate from a  
24 different direction with respect to the largest patches, as observed in the Parkfield

1 earthquakes in 1966 and 2004 (Bakun et al., 2005; Murray and Langbein, 2006). After  
2 the rupture of the largest patch, every rupture similarly propagates unilaterally to the  
3 lower part. The rupture directivity towards the bottom releases much stress at the  
4 bottom with respect to the top, which is known as the overshoot effect. This effect  
5 explains low seismicity in the lower part of the fault and precludes preparation to a  
6 characteristic event.

7 In contrast, large quasi-static nucleation areas with low stress appear before some  
8 characteristic events for maps (4) and (5) in Figure 8. In other words, this is a  
9 pre-slipped area and the stress concentration surrounding this area promotes the  
10 initiation of a large earthquake. The typical case is clearly seen in the third cycle of map  
11 (4). Here an earthquake of magnitude 5.7 occurs in early stage of the stress build-up  
12 (Figure 4) and this cannot grow further at this time. The seismicity in and around the  
13 ruptured area becomes high (Figure 7). In other words, the characteristic earthquake  
14 fails to occur following one favorable scenario and the system has to wait a long time  
15 for the next possible scenario (see the third characteristic earthquakes) when the system  
16 is highly charged and heterogeneous. This increases the seismicity (Figures 5 and 6),  
17 especially small earthquakes occurring in the surrounding area, which cannot become  
18 large enough to lead to a characteristic event (Figure 7). These are anomalies in the fault  
19 system, controlled by the timing of an intermediate earthquake.

20 Map (3) in Figure 8 shows similar characteristics to maps (1) and (2) although it has a  
21 slightly nonlinear G-R relation (Figure 6). The characteristic events always begin on the  
22 largest patch without interacting with the other large patches located in the  
23 middle-to-upper part. This means the coalescence of the smaller patches (light blue) is  
24 strong enough to break the largest ones. Another reason comes from the fact that the

1 patches in the upper part are not activated so favorably due to the directivity effect of  
2 the characteristic earthquake once this occurred on the lower part.

3 In this way, the anomalies found in the simulations can be understood while analyzing  
4 in detail the on-going earthquake sequence through the statistical features and the  
5 physical rupture processes. Therefore the scenario of the forth-coming characteristic  
6 earthquake in the concerned seismic cycle can be constrained with respect to its time,  
7 position and rupture directivity.

#### 9 **4. Discussion**

10  
11 We have observed that different heterogeneity maps with the same statistical features  
12 lead to a diversity of earthquake sequences, conserving some deterministic features of  
13 the characteristic earthquakes. Let us now consider the sensitivity to the parameters of  
14 the assumed rupture initiation process. The form of our probabilistic function (5) is  
15 hypothetical and the shape parameter  $k$  controls the sensitivity of initial rupture process  
16 to the loaded stress field, as demonstrated in Figure 3,. For easy comparison, we use the  
17 same maps as (1).

18 First Figure 9 shows a case for  $k = 3$  (Figure 3), where the earthquake initiation point is  
19 selected almost independently with respect to the stress distribution determined by the  
20 previous earthquake history. Therefore the earthquake distribution always remains  
21 almost uniform without any explicit localization (d). As a result, the number of smaller  
22 earthquakes increases in the size-frequency relation (Figure 9b-c).

23 Figure 10 shows the opposite case,  $k = 60$ , where rupture selectively starts from a patch  
24 of high stress accumulation and system behavior is significantly different. Since the

1 computation takes too long, we show only the first year starting with a uniform stress  
2 condition, which represents a typical behavior of this system. Very early earthquakes  
3 are dispersed over the fault, as the initial stress is uniform anywhere. However, soon the  
4 predominant earthquake sequence appears (bottom part of Figure 10d), where the  
5 following earthquakes occur only near the periphery of the previous rupture area. In the  
6 rest of the model space, the initiation probability (Figure 3) remains very low. This  
7 predominant sequence progresses very quickly, as earthquakes are triggered at almost  
8 every time step. Thus, the sequence shows a very concentrated time history, as seen in  
9 Figures 10(a) and (b), suggesting insufficient temporal resolution with the current time  
10 step. The extension of the ruptured area works as the quasi-static nucleation process and  
11 the characteristic earthquake occurs after the ruptured area becomes a critical size. The  
12 earthquake size distribution deviates from self-similar relation. In this example, the  
13 heterogeneous stress field generated rapidly by some initial earthquakes controls the  
14 following sequence. It also suggests that any anomaly in the initial stress field may  
15 control the whole earthquake sequence.

16 It is widely known that some cellular automaton models generate a Gutenberg-Richter  
17 like size-frequency distribution (e.g. Bak and Tang, 1989), while elastic continuum  
18 models with a characteristic length converge into a periodic behavior (e.g. Rice, 1993).  
19 Our system behavior cannot be interpreted using these two end members. Figure 9 and  
20 10 show that stochastic initiation process must be adjusted to mimic the vast distribution  
21 of the seismicity, characteristic earthquakes, and a Gutenberg-Richter relation. However,  
22 the essential part of our model is the heterogeneity map derived from Equations (1) –  
23 (3), as randomly initiated rupture on such a heterogeneous map gives a  
24 Gutenberg-Richter relation (Ide and Aochi, 2005) even without any system evolution.

1 As the introduction of system evolution sometimes interferes with the intrinsic features  
2 of the system, anomalies found in the current simulation might be hidden if we consider  
3 further complexity of the natural system.

4 Our general concern for natural earthquakes is how a characteristic earthquake appears  
5 in the seismic cycle. We assume built-in heterogeneous  $D_c$  distribution that is  
6 conserved after each characteristic event, which might be debatable. Probably the  
7 patches (fault heterogeneity) at larger scales is intrinsic (invariable in space) during a  
8 few seismic cycles, as inferred from the slip distributions of subsequent earthquakes in  
9 the subduction zones around Japan (Nagai et al. 2001, Yamanaka and Kikuchi, 2003)  
10 and at Parkfield (Murray and Langbein, 2006). In laboratory experiments, large  
11 asperities due to geometric irregularities are well conserved such that ruptures begin on  
12 the faults similarly (Ohnaka and Shen, 1999) and this matches with our initial model of  
13 multi-scale  $D_c$  (Ide and Aochi, 2005). As the initiation process at smaller scales in our  
14 simulation is stochastic, the earthquake sequences appearing at small scales seem  
15 different every time. Keeping the same heterogeneity at all scales may be acceptable as  
16 a first attempt. However, this point should be discussed further in future studies.

17 As mentioned earlier, the stochastic rupture initiation process can be debated because  
18 most of our observations concern the macroscopic fracture criterion. Without  
19 knowledge of the real dynamics and fine-scale heterogeneity in the first instability scale,  
20 such a stochastic description would be a practical substitute. Then, our current  
21 normalization process homogenizes the initial field information during the rupture  
22 propagation. This is correct at the scale of characteristic earthquakes, but it will be  
23 another interesting topic to study how smaller heterogeneity influences the rupture

1 process at each scale. Fine-scale complexity around the rupture front may generate very  
2 complex seismic wave radiation at high frequencies. Such processes will require further  
3 numerical developments, such as auto-adopted gridding within the BIEM.

## 5. Summary

7 A sequence of complex dynamic rupture events under a constant tectonic loading is  
8 simulated based on a multi-scale heterogeneous fault model with circular patches, a  
9 stochastic rupture initiation process governed by a Weibull probabilistic function and  
10 instantaneous healing of the fault strength by keeping the same map during every cycle.

11 The simulation results are analyzed statistically to explain their diversity and their  
12 similarity both from the statistics of the seismicity and from the physical process of the  
13 earthquake rupture. As previously shown in Ide and Aochi (2005), a self-organized  
14 system such as the Gutenberg-Richter size distribution relation originates from the  
15 multi-scale heterogeneity map we assume. However, different simulations show that the  
16 history of stress field may hide this intrinsic feature. The diversity of earthquake  
17 sequences is principally controlled by the spatial distribution of the patches. Although  
18 the exact time and position of the onset of the characteristic earthquakes cannot be  
19 predicted, they occur rather regularly in time and similarly in different seismic cycles.

20 Dynamic rupture processes of the characteristic earthquakes leave heterogeneous  
21 residual stresses due to directivity and overshoot effects, so that this pattern often  
22 controls the spatial distribution of the following seismicity. It is also found that larger  
23 earthquakes may occur later in each seismic cycle. This means much stress  
24 concentration over large area is required for a rupture to propagate spontaneously to a

1 larger area. Some irregular characteristic earthquakes may occur based on the map and  
2 the randomness of the preceding earthquake sequence. In this case, an anomaly in the  
3 seismicity such as the number of earthquakes, size distribution and spatial distribution  
4 becomes visible. From the physical viewpoint, this is due to an intermediate earthquake  
5 before the stress is sufficiently accumulated over the fault system. This means that such  
6 an anomaly is not predictable before the cycle, but understandable through the analysis  
7 of the concerned earthquakes during the cycle. In nature no fault system can be isolated  
8 from the others, so that the phenomena should be more complex. However, the  
9 similarity and the diversity simulated in this study, governed by the structure of an  
10 inherent distribution of  $D_c$ , suggests the importance of pre-existing fault heterogeneity  
11 structure for the appearance of earthquake sequences, including those that are  
12 characteristic.

13

## 14 **Acknowledgments**

15

16 We thank Martin Mai, Sandy Steacy and a few anonymous reviewers for their critical  
17 comments on our manuscript. Some of them encouraged us to test different  
18 heterogeneous maps to improve our comprehension and discussion. We also thank John  
19 Douglas for reviewing our revised manuscript. H.A. receives partial financial support  
20 from the French national project INSU 3F - Rhéologie des asperities de faille (2007).  
21 The parallel calculations were carried out in the Digital Information Systems Division  
22 of the BRGM. This study is a contribution to BRGM's research program on seismic risk.  
23 This work is also partially supported by Ministry of Education, Culture, Sports, Science  
24 and Technology (MEXT), Japan.

## References

1. Andrews, D. J. (1976), Rupture propagation with finite stress in antiplane strain, *J. Geophys. Res.*, 81, 3575-3582.
2. Andrews, D. J. (2005), Rupture dynamics with energy loss outside the slip zone, *J. Geophys. Res.*, 110, doi:10.1029/2004JB003191.
3. Aochi, H. and E. Fukuyama (2002), Three-dimensional nonplanar simulation of the 1992 Landers earthquake, *J. Geophys. Res.*, 107, doi:10.1029/2000JB000061.
4. Aochi, H. and S. Ide (2004), Numerical study on multi-scaling earthquake rupture, *Geophys. Res. Lett.*, 31, L02606, doi:10.1029/2003GL018708.
5. Aochi, H., M. Cushing, O. Scotti, and C. Berge-Thierry (2006), Estimating rupture scenario likelihood based on dynamic rupture simulations: the example of the segmented Middle Durance fault, southeastern France, *Geophys. J. Int.*, 165, 436-446.
6. Atkinson, B. K. (1984), Subcritical crack growth in geological materials, *J. Geophys. Res.*, 89(B6), 4077-4114.
7. Bak, P. and C. Tang (1989), Earthquakes as a self-organized critical phenomenon, *J. Geophys. Res.*, 94, 15635-15637.
8. Bakun, W. H., B. Aagaard, B. Dost, W. L. Ellsworth, J. L. Hardebeck, R. A. Harris, C. Ji, M. J. S. Johnston, J. Langbein, J. J. Lienkaemper, A. J. Michael, J. R. Murray, R. M. Nadeau, P. A. Reasenber, M. S. Reichle, E. A. Roeloffs, A. Shakal, R. W. Simpson, and F. Waldhauser (2005), Implications for prediction and hazard assessment from the 2004 Parkfield earthquake, *Nature*, 437, 969-974.

- 1 9. Ben-Zion, Y. and J. R. Rice (1993), Earthquake failure sequences along a  
2 cellular fault zone in a 3-dimensional elastic solid containing asperity and  
3 nonasperity regions, *J. Geophys. Res.*, 98, 14109-14131.
- 4 10. Beroza, G. and P. Spudich (1988), Linearized inversion for fault rupture  
5 behavior: Application to the 1984 Morgan Hill, California, earthquake, *J.*  
6 *Geophys. Res.*, 93, 6275-6296.
- 7 11. Das, S. and K. Aki (1977), A numerical study of two-dimensional spontaneous  
8 rupture propagation, *Geophys. J. R. Astron. Soc.*, 50, 643-668.
- 9 12. Duan, B. and D. D. Oglesby (2005), Multicycle dynamics of nonplanar  
10 strike-slip faults, *J. Geophys. Res.*, 110, B03304, doi:10.1029/2004JB003298.
- 11 13. Ellsworth, W. L. and G. C. Beroza (1995), Seismic evidence for an earthquake  
12 nucleation phase, *Science*, 268, 851-855.
- 13 14. Guatteri, M., P. M. Mai, G. C. Beroza and J. Boatwright (2003), Strong-ground  
14 motion prediction from stochastic-dynamic source models, *Bull. Seism. Soc.*  
15 *Am.*, 93, pp301-313.
- 16 15. Hillers, G., Y. Ben-Zion and P. M. Mai (2006), Seismicity on a fault controlled  
17 by rate- and state-dependent friction with spatial variations of the critical slip  
18 distance, *J. Geophys. Res.*, 111, doi:10.1029/2005JB003859.
- 19 16. Ide, S. (2002), Estimation of radiated energy of finite-source earthquake models,  
20 *Bull. Seismol. Soc. Am.* 92, 2294-3005.
- 21 17. Ide, S. and H. Aochi (2005), Earthquakes as multiscale dynamic ruptures with  
22 heterogeneous fracture surface energy, *J. Geophys. Res.*, 110, B11303,  
23 doi:10.1029/2004JB003591.
- 24 18. Ide, S. and G. C. Beroza (2001), Does apparent stress vary with earthquake size?,

- 1           Geophys. Res. Lett., 28, 3349-3352.
- 2           19. Fukuyama, E. and R. Madariaga (1998), Rupture dynamics of a planar fault in a  
3           3D elastic medium: Rate- and slip-weakening friction, *Bull. Seismol. Soc. Am.*,  
4           88, 1-17.
- 5           20. Fukuyama, E. and R. Madariaga (1995), Integral equation method for plane  
6           crack with arbitrary shape in 3D elastic medium, *Bull. Seismol. Soc. Am.*, 85,  
7           614-628.
- 8           21. Lapusta, N. and Y. Liu (2008), 3D boundary-integral modeling of spontaneous  
9           earthquake sequences and aseismic slip, in press, *J. Geophys. Res.*
- 10          22. Lapusta, N., J. R. Rice, Y. Ben-Zion and G. Zheng (2000), Elastodynamic  
11          analysis for slow tectonic loading with spontaneous rupture episodes on faults  
12          with rate- and state-dependent friction, *J. Geophys. Res.*, 105, 23765-23789.
- 13          23. Madariaga, R. and K. B. Olsen (2000), Criticality of rupture dynamics in 3D,  
14          *Pure Appl. Geophys.*, 157, 1981-2001.
- 15          24. Mai, P. M., P. Somerville, A. Pitarka, L. Dalguer, S. Song, G. Beroza, H.  
16          Miyake and K. Irikura (2006), On scaling of fracture energy and stress drop in  
17          dynamic rupture models : Consequences for near-source ground motions, in  
18          *Earthquake : Radiated energy and the physics of faulting*, Geophysical  
19          Monograph Series 170, 283-293.
- 20          25. Mikumo, T. and T. Miyatake (1983), Numerical modeling of space and time  
21          variations of seismic activity before major earthquakes, *Geophys. J. R. astr. Soc.*,  
22          74, 559-583.
- 23          26. Mikumo, T. and T. Miyatake (1979), Earthquake sequences on a frictional fault  
24          model with non-uniform strengths and relaxation times, *Geophys. J. R. Astr.*

- 1 Soc., 59, 497-522.
- 2 27. Mikumo, T. And T. Miyatake (1978), Dynamic rupture process on a  
3 three-dimensional fault with non-uniform frictions and near-field seismic waves,  
4 Geophys. J. R. Astr. Soc., 54, 417-438.
- 5 28. Murray, J. and J. Langbein (2006), Slip on the San Andreas Fault at Parkfield,  
6 California, over Two Earthquake Cycles, and the Implications for Seismic  
7 Hazard, Bull. Seismol. Soc. Am., 96, S283-S303.
- 8 29. Nagai, R., M. Kikuchi, and Y. Yamanaka (2001), Comparative study on the  
9 source process of recurrent large earthquakes in Sanriku-oki region: the 1968  
10 Tokachi-oki earthquake and the 1994 Sanriku-oki earthquake, *Zishin*, 54,  
11 267-280 (in Japanese with English abstract).
- 12 30. Oglesby, D. D. and S. M. Day (2002), Stochastic fault stress: Implications for  
13 fault dynamics and ground motion, Bull. Seism. Soc. Am., 92, 3022-3041.
- 14 31. Olsen, K. B., R. Madariaga and R. J. Archuleta (1997), Three-dimensional  
15 dynamic simulation of the 1992 Landers earthquake, *Science*, 278, 834-838.
- 16 32. Ohnaka, M. and L. Shen (1999), Scaling of the shear rupture process from  
17 nucleation to dynamic propagation: Implications of geometric irregularity of the  
18 rupturing surfaces, *J. Geophys. Res.*, 104(B1), 817-844.
- 19 33. Otsuka, M. (1971), A simulation earthquake occurrence Part 1, A mechanical  
20 model, *J. Seis. Soc. Jpn*, 24, 13-25.
- 21 34. Ripperger, J., J. P. Ampuero, P. M. Mai and D. Giardini (2007), Earthquake  
22 source characteristics from dynamic rupture with constrained stochastic fault  
23 stress, *J. Geophys. Res.*, 112, doi:10.1029/2006JB004515.
- 24 35. Rice, J. R. (1993), Spatio-temporal Complexity of Slip on a Fault, *J. Geophys.*

- 1           Res., 98, 9885-9907.
- 2           36. Shaw, B. E. and J. H. Dieterich (2007), Probabilities for jumping fault segment  
3           stopovers, *Geophys. Res. Lett.*, 34, L01307, doi:10.1029/2006GL027980.
- 4           37. Shibazaki, B. and M. Matsu'ura (1998), Transition process from nucleation to  
5           high-speed rupture propagation: scaling from stick-slip experiments to natural  
6           earthquakes, *Geophys. J. Int.*, 132, 14-30.
- 7           38. Uchide, T. and S. Ide (2007), Development of multiscale slip inversion method  
8           and its application to the 2004 mid-Niigata Prefecture earthquake, *J. Geophys.*  
9           *Res.*, 112, B06313, doi:10.1029/2006JB004528.
- 10          39. Yamaguchi, Y. and U. Nishimatsu (1967), Introduction to rock mechanics,  
11          Tokyo University Press (in Japanese).
- 12          40. Yamanaka, Y. and M. Kikuchi (2003), Source processes of the recurrent  
13          Tokachi-oki earthquake on September 26, 2003, inferred from teleseismic body  
14          waves, *Earth Planets Space*, 55, e21–e24.
- 15          41. Yamashita, T. (1993), Application of fracture mechanics to the simulation of  
16          seismicity and recurrence of characteristic earthquakes on a fault, *J. Geophys.*  
17          *Res.*, 98, 12019-12032.
- 18          42. Yamashita, T. and E. Fukuyama (1996), Apparent critical slip displacement  
19          caused by the existence of a fault zone, *Geophys. J. Int.*, 125, 459-472.
- 20          43. Zöller, G., S. Hainzl, M. Holschneider and Y. Ben-Zion (2005a), Aftershocks  
21          resulting from creeping sections in a heterogeneous fault, *Geophys. Res., Lett.*,  
22          32, doi:10.1029/2004GL021871.
- 23          44. Zöller, G., M. Holschneider and Y. Ben-Zion (2005b), The role of heterogeneity  
24          as a tuning parameter of earthquake dynamics, *Pure Appl. Geophys.*, 162,

1 1027-1049.

2

1

| Parameter                                | Quantity                |
|--|-------------------------|
| Rigidity                                 | 32.4 Gpa                |
| P-wave velocity                          | 6000 m/s                |
| S-wave velocity                          | 3464 m/s                |
| BIEM grid size                           | 4 m at minimum          |
| BIEM time step                           | 0.33 ms at minimum      |
| Peak strength $\Delta\tau_b$             | 5 MPa                   |
| Critical slip distance $D_c$             | Variable (See Figure 2) |
| Weibull's shape parameter $k$            | 15                      |
| Weibull's scale parameter $\lambda$      | 5 MPa                   |
| Period $T$                               | 20 years                |
| Event probability $P_{event}$            | 0.1 per hour            |
| Tectonic loading $\Delta\tau_{tectonic}$ | 10 Pa per hour          |

2 **Table 1: Model parameters used in the simulations.**

3

1

| Fault Heterogeneity Map         | (1)   | (2)   | (3)   | (4)   | (5)   | Max (Tr) | Min (Tr) | Max(Tr)-Min(Tr) |
|---------------------------------|-------|-------|-------|-------|-------|----------|----------|-----------------|
| Average Recurrence Time :Tr(yr) | 19.61 | 20.12 | 20.92 | 21.07 | 19.18 | 21.07    | 19.18    | 1.89            |
| Max (Tr)                        | 19.99 | 20.25 | 21.34 | 21.88 | 21.10 |          |          |                 |
| Min (Tr)                        | 19.05 | 19.85 | 20.36 | 20.41 | 18.58 |          |          |                 |
| Max(Tr)-Min(Tr)                 | 0.94  | 0.40  | 0.98  | 1.46  | 2.52  |          |          |                 |

2

3

4

5

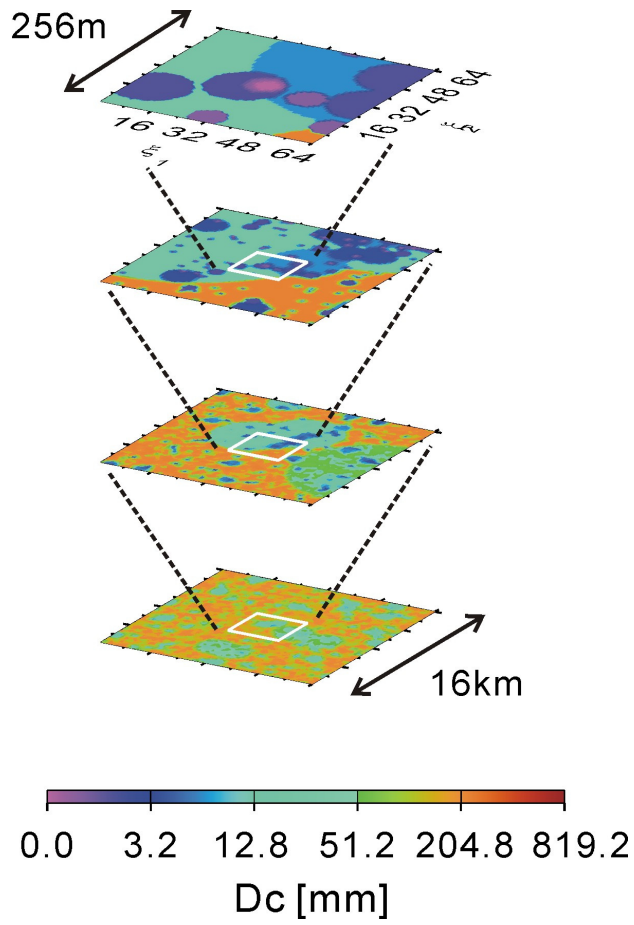
6

7

8

**Table 2: Recurrence time of the simulated characteristic earthquakes for each fault heterogeneity map. To the bottom, the maximum, the minimum and their difference are presented for each map. To the right, the maximum, the minimum and the difference are calculated for the averages of each simulation.**

1

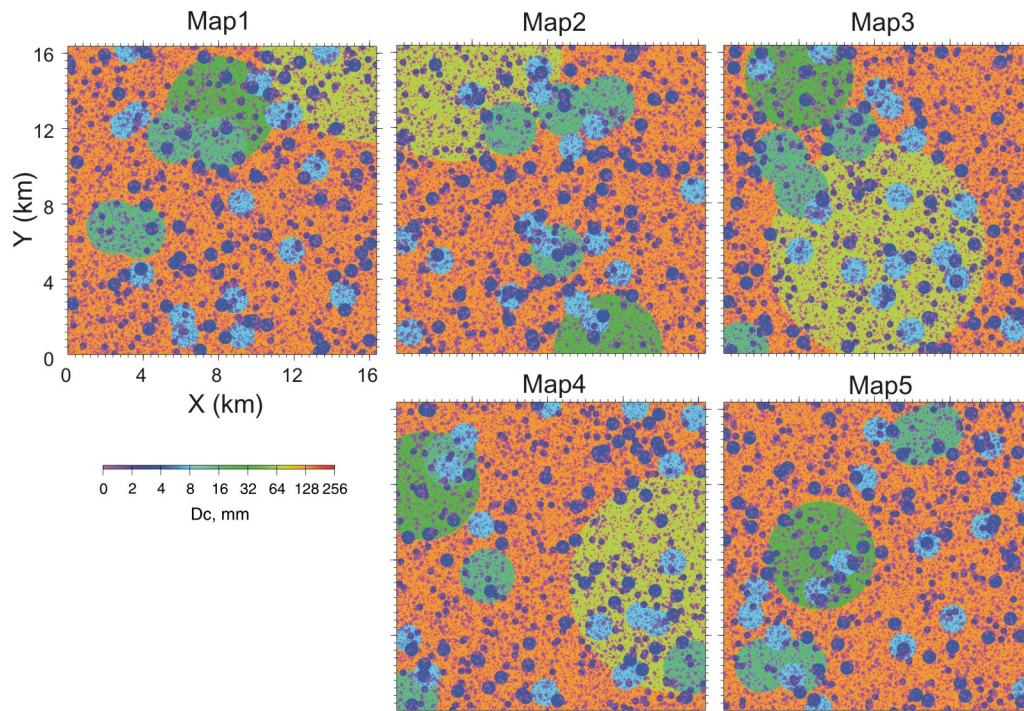


2

3

4 **Figure 1. Schematic illustration of multi-scale heterogeneous  $D_c$  distribution [after Ide and**  
5 **Aochi (2005)]. Focusing on the microscopic scale, one finds numerous small parts of small**  
6  **$D_c$ .**

1



2

3

4

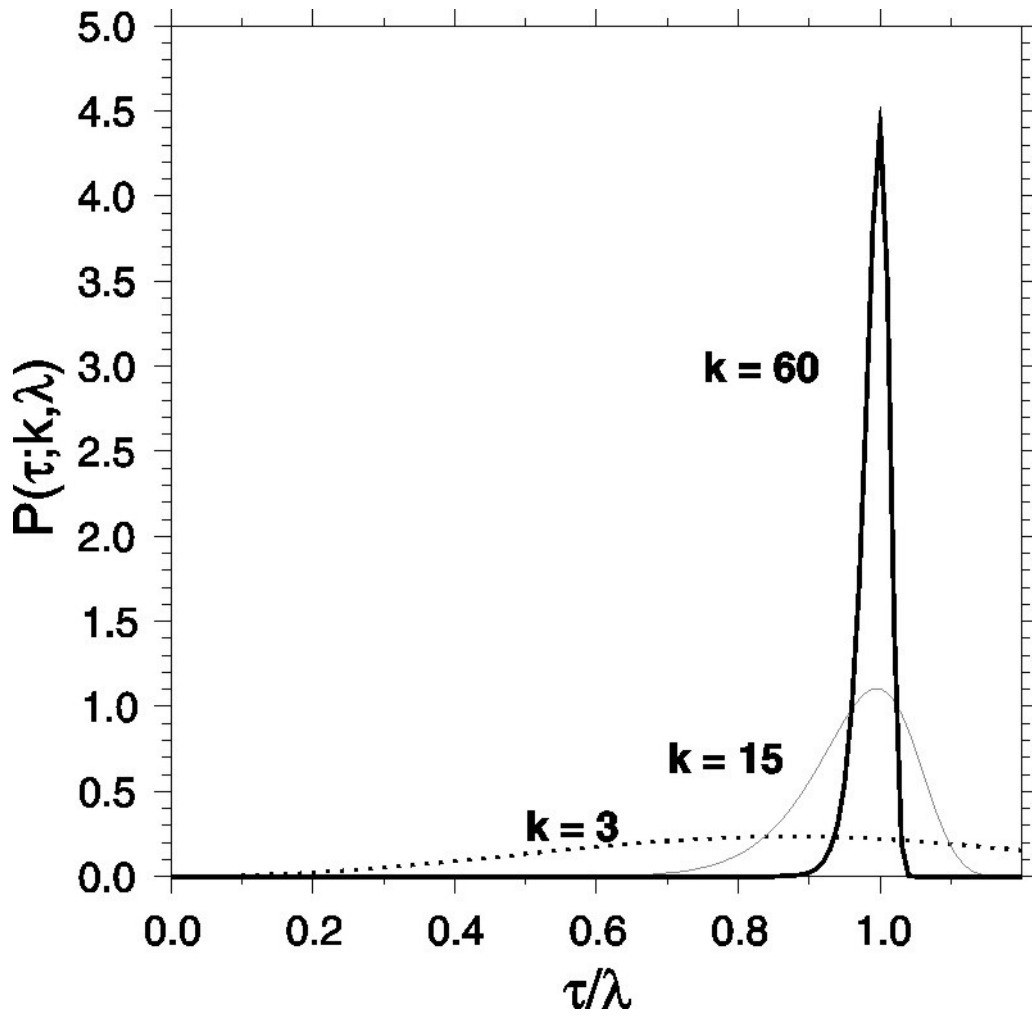
5

6

7

Figure 2: Five heterogeneity maps stochastically generated according to the same rules. The model area (X, Y) has a dimension of 16384 m x 16384 m, namely 4096 x 4096 grids in the minimum scale. The appearance probability of the maximum patch (olive) is 0.25, so that it is possible that this patch does not appear in the area as in Map 5. See the text in the detail.

1

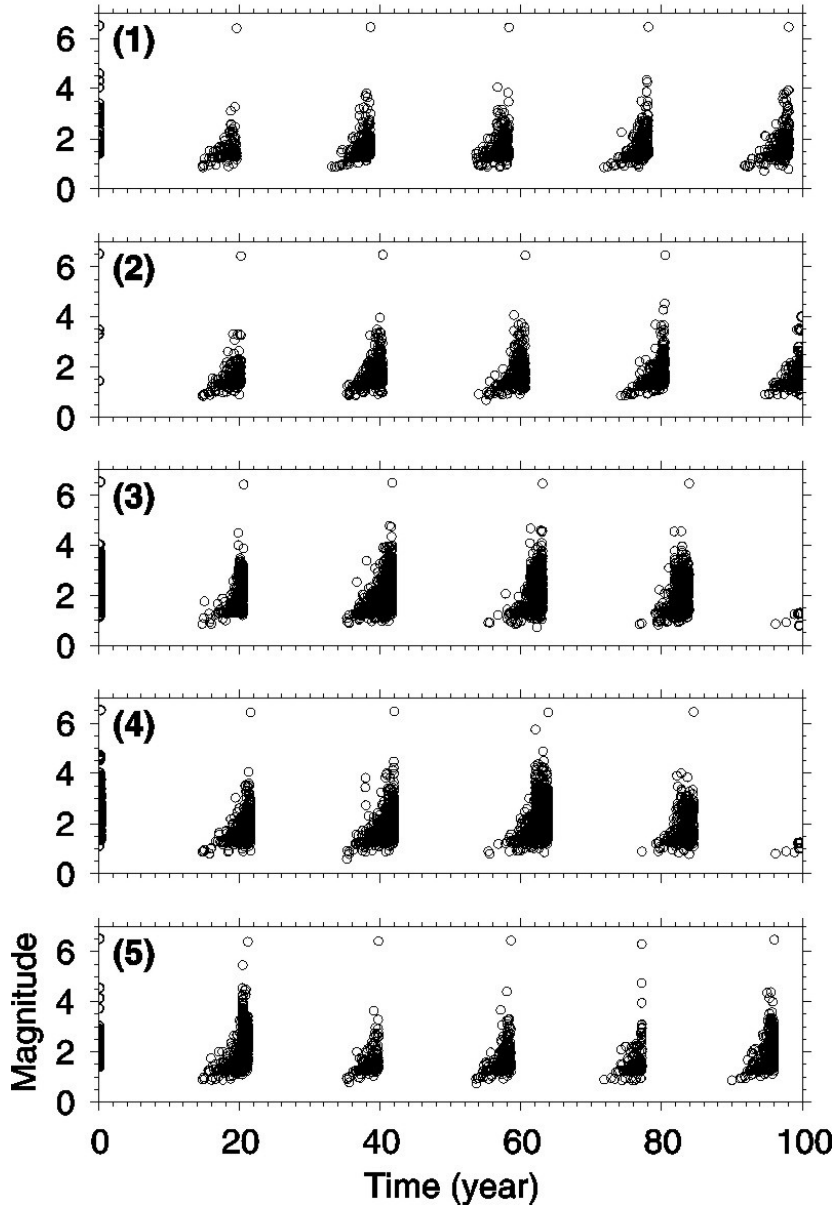


2  
3  
4  
5  
6

Figure 3: Probabilistic function defined by Equation (5) for  $k = 3, 15$  and  $60$ .

1

## Seismicity during 100 years



2

3

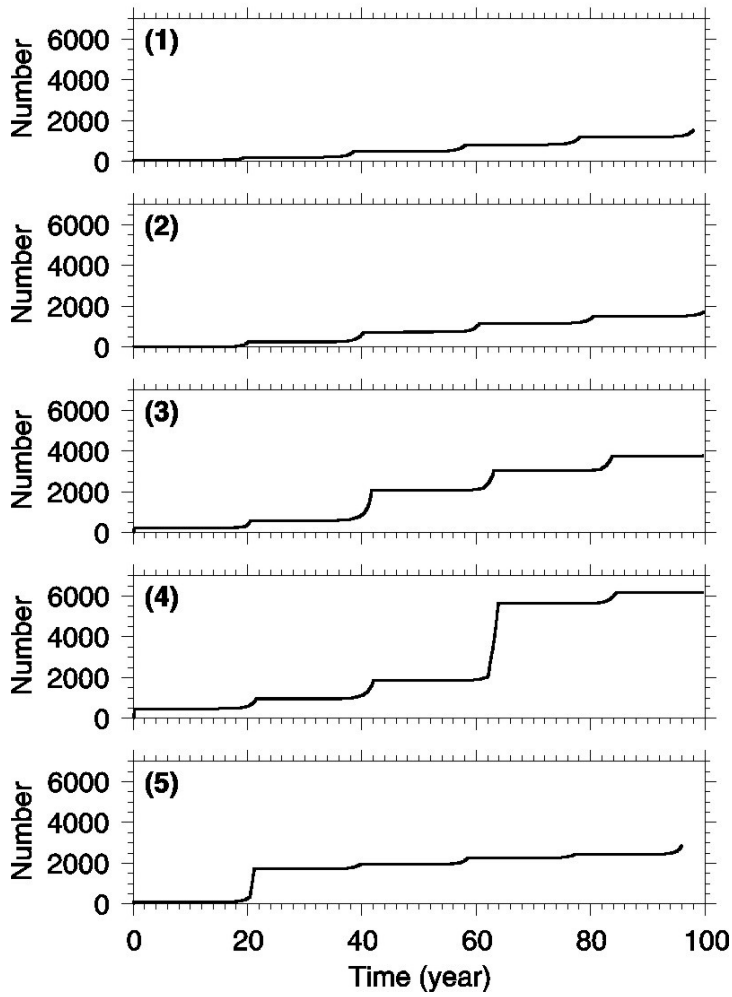
4

5

Figure 4: Earthquake sequences with time for each heterogeneity map. The number in the upper left corner corresponds to the number of each map.

1

### Cumulative Number



2

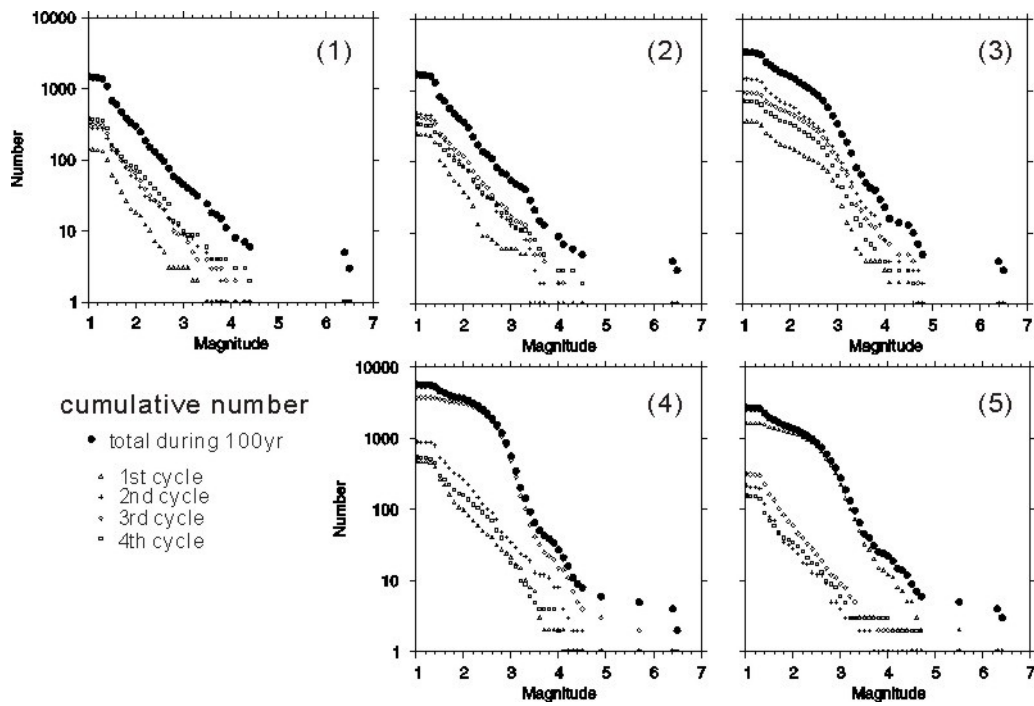
3

4

5

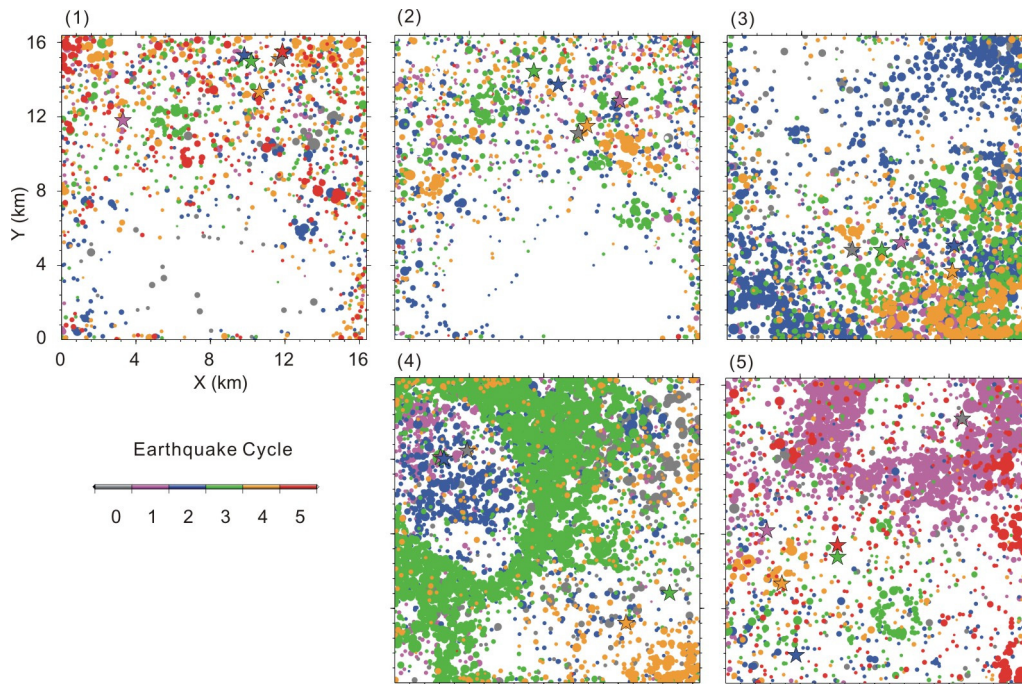
6

Figure5: Cumulative number of earthquakes with time for each map, (1) to (5). The curves in (1) and (5) end just before 100 years, because there is no seismicity following the previous characteristic earthquakes.



1  
 2 Figure 6: Earthquake numbers against magnitude for each map from (1) to (5). The black circle shows the  
 3 total seismicity during 100 years of each simulation. Other marks represent four cycles within the 100  
 4 years.

1



2

3

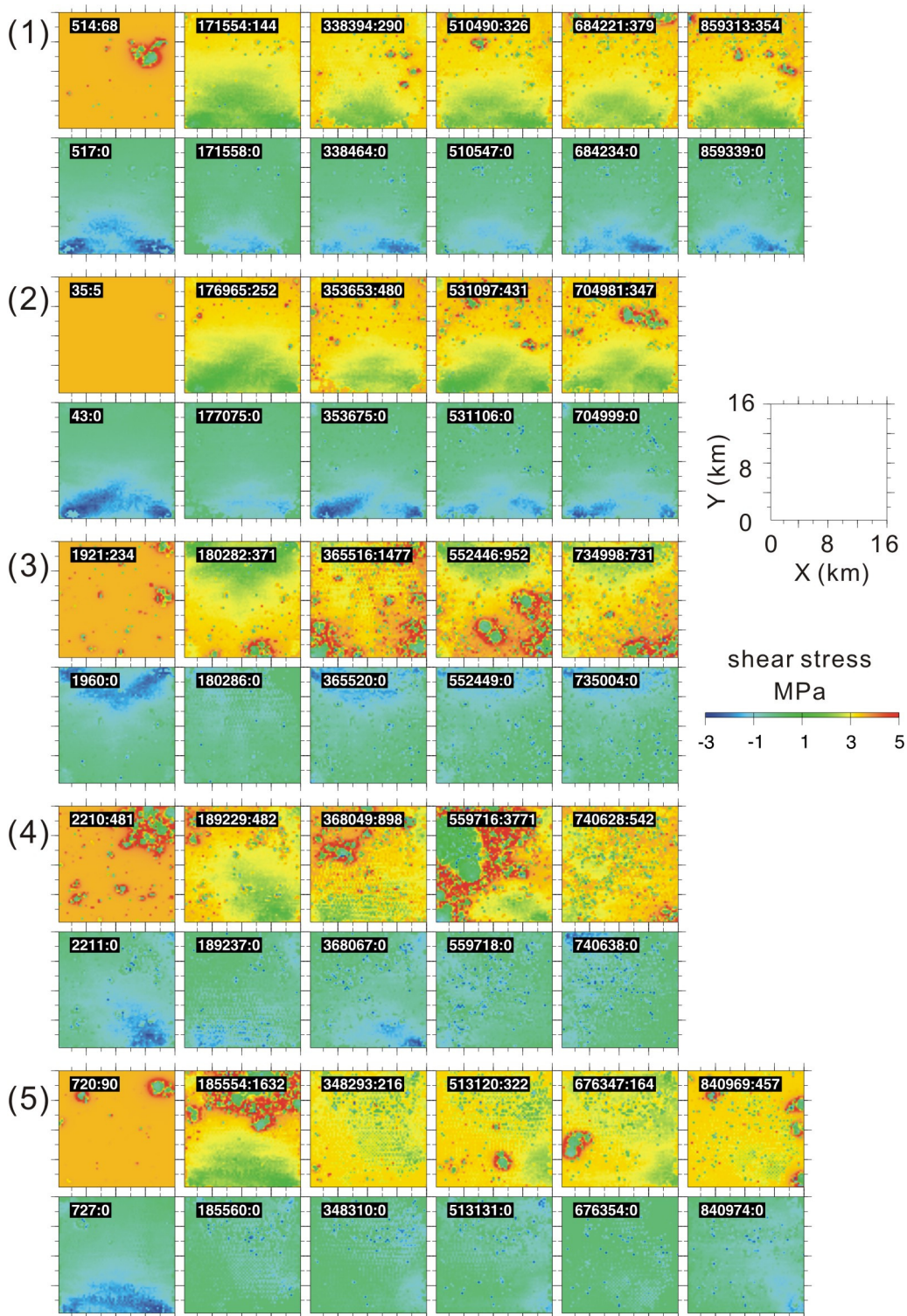
4

5

6

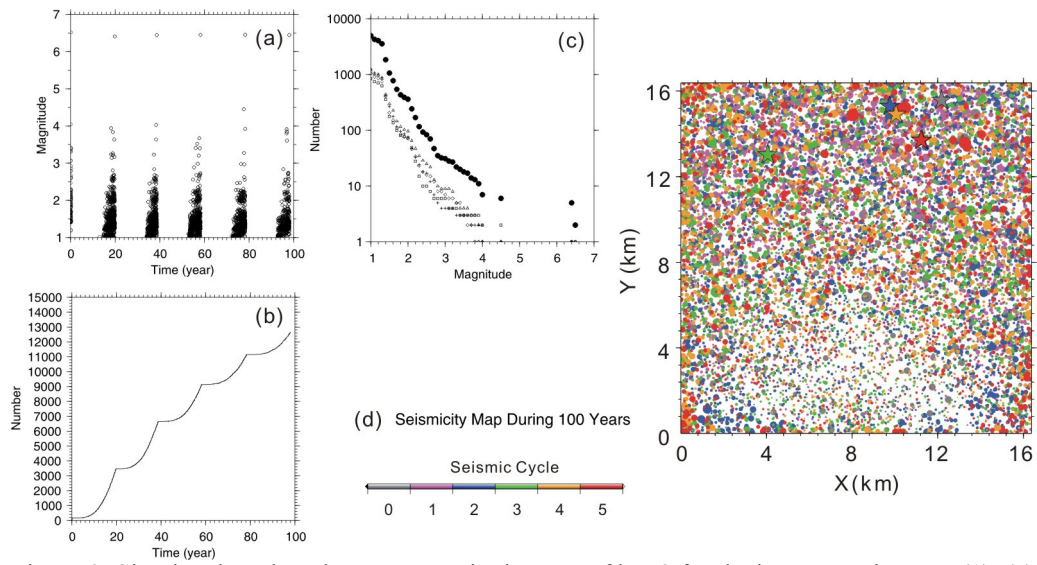
7

**Figure 7: Spatial distribution of hypocenters of earthquake sequences during the simulated 100 years. Events are plotted by different colors according to the seismic cycles, each of which ends with the characteristic event represented by stars. The size of circles is proportional to the event magnitude, but it does not represent the physically ruptured area.**

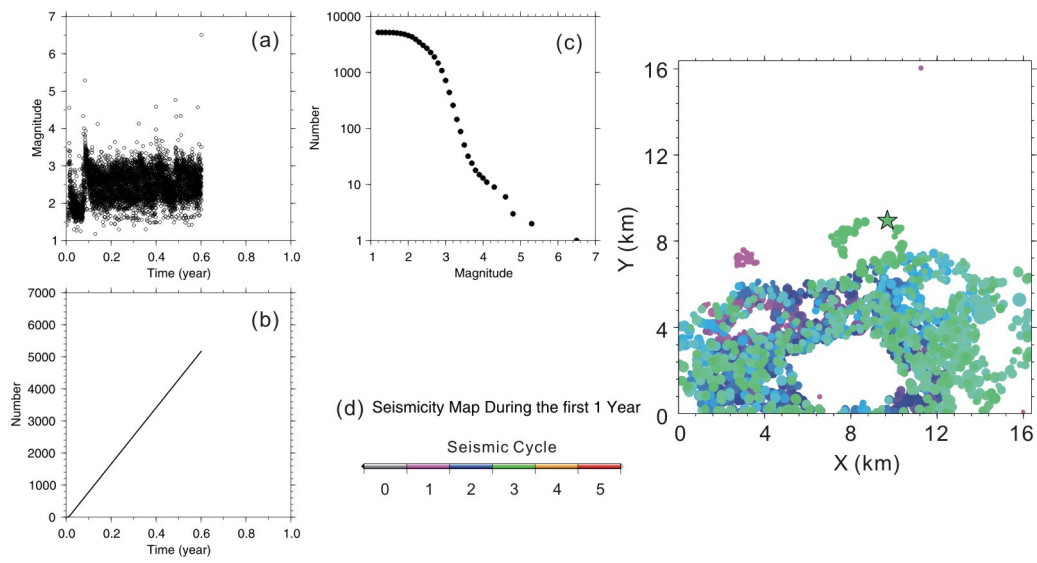


1  
2  
3  
4  
5  
6  
7

Figure 8: Stress field on the whole fault area before (upper row) and after (lower row) the characteristic earthquakes of each simulation (1) to (5). It should be made clear that the upper row corresponds to the earthquake preceding the characteristic event. The numbers separated by a colon represent, respectively, the event time in hours and the sequence number in each cycle (0 for the characteristic one). Each panel shows the entire fault regions of 16.4 km x 16.4 km.



1  
 2 Figure 9: Simulated earthquake sequences in the case of  $k = 3$  for the heterogeneity map (1). (a)  
 3 Magnitude-Time, (b) Earthquake cumulative number – Time, (c) Size distribution and (d) Hypocenter  
 4 distribution. See also the captions of the previous figures.



1  
2  
3  
4  
5

Figure 10: Simulated earthquake sequences for  $k = 60$  on the heterogeneity map (1). Cumulative earthquake number against magnitude on the left panel and stress evolution for every 200 events in right panel.